



HAL
open science

Thermally induced magnetization switching in Fe/MnAs/GaAs(001): selectable magnetic configurations by temperature and field control

Carlo Spezzani, Franck Vidal, Renaud Delaunay, Mahmoud Eddrief,
Massimiliano Marangolo, Victor H. Etgens, Horia Popescu, Maurizio Sacchi

► **To cite this version:**

Carlo Spezzani, Franck Vidal, Renaud Delaunay, Mahmoud Eddrief, Massimiliano Marangolo, et al.. Thermally induced magnetization switching in Fe/MnAs/GaAs(001): selectable magnetic configurations by temperature and field control. *Scientific Reports*, 2015, 5, pp.8120. 10.1038/srep08120 . hal-01223188

HAL Id: hal-01223188

<https://hal.sorbonne-universite.fr/hal-01223188v1>

Submitted on 3 Nov 2015

HAL is a multi-disciplinary open access archive for the deposit and dissemination of scientific research documents, whether they are published or not. The documents may come from teaching and research institutions in France or abroad, or from public or private research centers.

L'archive ouverte pluridisciplinaire **HAL**, est destinée au dépôt et à la diffusion de documents scientifiques de niveau recherche, publiés ou non, émanant des établissements d'enseignement et de recherche français ou étrangers, des laboratoires publics ou privés.



Distributed under a Creative Commons Attribution - NonCommercial - ShareAlike 4.0 International License



OPEN

SUBJECT AREAS:
MAGNETIC PROPERTIES
AND MATERIALS
MAGNETIC DEVICESReceived
20 October 2014Accepted
2 January 2015Published
29 January 2015Correspondence and
requests for materials
should be addressed to
M.S. (maurizio.
sacchi@insp.jussieu.fr;
maurizio.sacchi@
synchrotron-soleil.fr)

Thermally induced magnetization switching in Fe/MnAs/GaAs(001): selectable magnetic configurations by temperature and field control

Carlo Spezzani¹, Franck Vidal^{2,3}, Renaud Delaunay^{4,5}, Mahmoud Eddrief^{2,3}, Massimiliano Marangolo^{2,3}, Victor H. Etgens^{2,3,6}, Horia Popescu⁷ & Maurizio Sacchi^{2,3,7}¹ELETTRA Sincrotrone Trieste, S.S. 14, Km 163.5, 34012, Trieste, Italy, ²Sorbonne Universités, UPMC Univ Paris 06, UMR 7588, INSP, 75005, Paris, France, ³CNRS, UMR 7588, Institut des NanoSciences de Paris, 75005, Paris, France, ⁴Sorbonne Universités, UPMC Univ Paris 06, UMR 7614, LCPMR, 75005 Paris, France, ⁵CNRS, UMR 7614, LCPMR, 75005 Paris, France, ⁶Institut VeDeCoM – UVSQ, 78000 Versailles, France, ⁷Synchrotron SOLEIL, B.P. 48, 91192 Gif-sur-Yvette, France.

Spintronic devices currently rely on magnetization control by external magnetic fields or spin-polarized currents. Developing temperature-driven magnetization control has potential for achieving enhanced device functionalities. Recently, there has been much interest in thermally induced magnetisation switching (TIMS), where the temperature control of intrinsic material properties drives a deterministic switching without applying external fields. TIMS, mainly investigated in rare-earth–transition-metal ferrimagnets, has also been observed in epitaxial Fe/MnAs/GaAs(001), where it stems from a completely different physical mechanism. In Fe/MnAs temperature actually modifies the surface dipolar fields associated with the MnAs magnetic microstructure. This in turn determines the effective magnetic field acting on the Fe overlayer. In this way one can reverse the Fe magnetization direction by performing thermal cycles at ambient temperatures. Here we use element selective magnetization measurements to demonstrate that various magnetic configurations of the Fe/MnAs/GaAs(001) system are stabilized predictably by acting on the thermal cycle parameters and on the presence of a bias field. We show in particular that the maximum temperature reached during the cycle affects the final magnetic configuration. Our findings show that applications are possible for fast magnetization switching, where local temperature changes are induced by laser excitations.

Controlling the local magnetization direction in a thin film without applying external magnetic fields is of considerable interest for designing new sensors and storage devices. Electric fields^{1,2}, spin-polarized currents^{3,4} and temperature control^{5,6} have been invoked as alternative ways of acting on the magnetization. Thermally induced magnetization switching (TIMS) has been investigated mainly in rare-earth transition-metal oxides^{5,6}, where magnetization reversal is achieved by using ultra-fast laser pulses, in an all-optical switching process^{7–9}. We have put forward an alternative approach to the manipulation of the magnetic properties of an overlayer, based on a magnetically active template¹⁰, i.e. using substrates whose intrinsic magnetic properties feature regular spatial modulations generating local surface dipolar fields that can be controlled by tuning external parameters, in particular temperature. Thin epitaxial MnAs layers grown on GaAs(001) belong to this class of materials¹¹.

Bulk MnAs features, at 40°C, a first order phase transition between the ferromagnetic α -phase and the paramagnetic β -phase^{12,13}, providing interesting magneto-caloric properties^{14–18}. When MnAs is grown epitaxially on GaAs(001), the two phases coexist over an extended range of ambient temperatures (~ 12 – 40°C), forming a regular set of alternating α and β stripes^{19–20}. The MnAs layer thickness determines the period of the stripes and the height of the steps separating them^{21–23}, while the relative width of α and β components within a period vary continuously with temperature^{21,23,24}. MnAs/GaAs(001) is a metal/semiconductor system that has potential in spintronic applications^{25–30}. In the past, we have studied the temperature dependence of its morphological and magnetic properties^{24,31}, and we used it as a template for growing an Fe ferromagnetic overlayer^{11,32,33}. We showed that by finely tuning the temperature at ambient it is possible to reverse the Fe magnetization in Fe/MnAs/



GaAs(001) without applying fields¹¹, a process with potential for applications in TIMS¹⁰. What we actually do by changing the temperature is control the surface dipolar fields associated with the MnAs template magnetic microstructure, and, ultimately, vary the effective magnetic field acting on the Fe overlayer^{11,34}.

In this work we analyze the role of both the temperature range spanned by the thermal cycle and of the presence of a bias magnetic field on the final magnetic configuration in Fe/MnAs/GaAs(001). In particular, we show that the maximum temperature reached in the thermal cycle can profoundly affect the final magnetic state, a result that may hamper applications based on using laser pulses as the heat source^{35–37}, since in that case the local maximum temperature is difficult to predict and control. We provide also a possible solution to this problem, since we demonstrate that by varying the strength of the bias field one can select the final stable magnetic configuration, regardless of the extent of the thermal cycle. Both results are relevant to all-optical switching and heat-assisted magnetization control.

Experimentally, we use x-ray reflectivity to probe the Fe and MnAs magnetic properties selectively. We achieve this by tuning the energy of the circularly polarized x-rays to the 2p-3d resonance of either Mn or Fe. This provides magnetization sensitivity and element selectivity³⁸, in addition to the large probing depth typical of a photon-in-photon-out x-ray experiment.

Results

Hysteresis loops and TIMS. First, we set out to show that our samples behave in the same way as systems previously studied^{11,32,33} in terms of temperature dependent hysteresis loops and magnetization switching. As yet, these kinds of result are not so common, and we consider it important to show them for the specific samples under consideration. This provides also an opportunity to discuss the Fe magnetization switching mechanism in more detail.

By tuning the energy of the circularly polarized x-rays to the Mn-2p (~640 eV) or to the Fe-2p (~707 eV) resonances, the reflected intensity is sensitive to the average magnetic moment carried by Mn atoms or by Fe atoms, respectively³³. As shown in Fig. 1, this element selectivity is essential for disentangling MnAs and Fe contributions and for an independent analysis of their magnetization behaviour. Although we are not interested here in determining absolute values of the Fe and MnAs magnetizations³⁸, but only their dependence on the external magnetic field and on the temperature, it is worth noticing that the proportionality constant between measured magnetic signals and the actual magnetization depends on the experimental conditions and it is not the same for Fe and Mn.

Fig. 1 shows hysteresis loops measured element selectively in sample A whose structure is Fe_{3nm}/MnAs_{200nm}/GaAs(001). At T = 7°C (Fig. 1a, MnAs in its α-phase), both Fe and Mn feature fairly square loops, with a remanent parallel (P) alignment between Fe and Mn

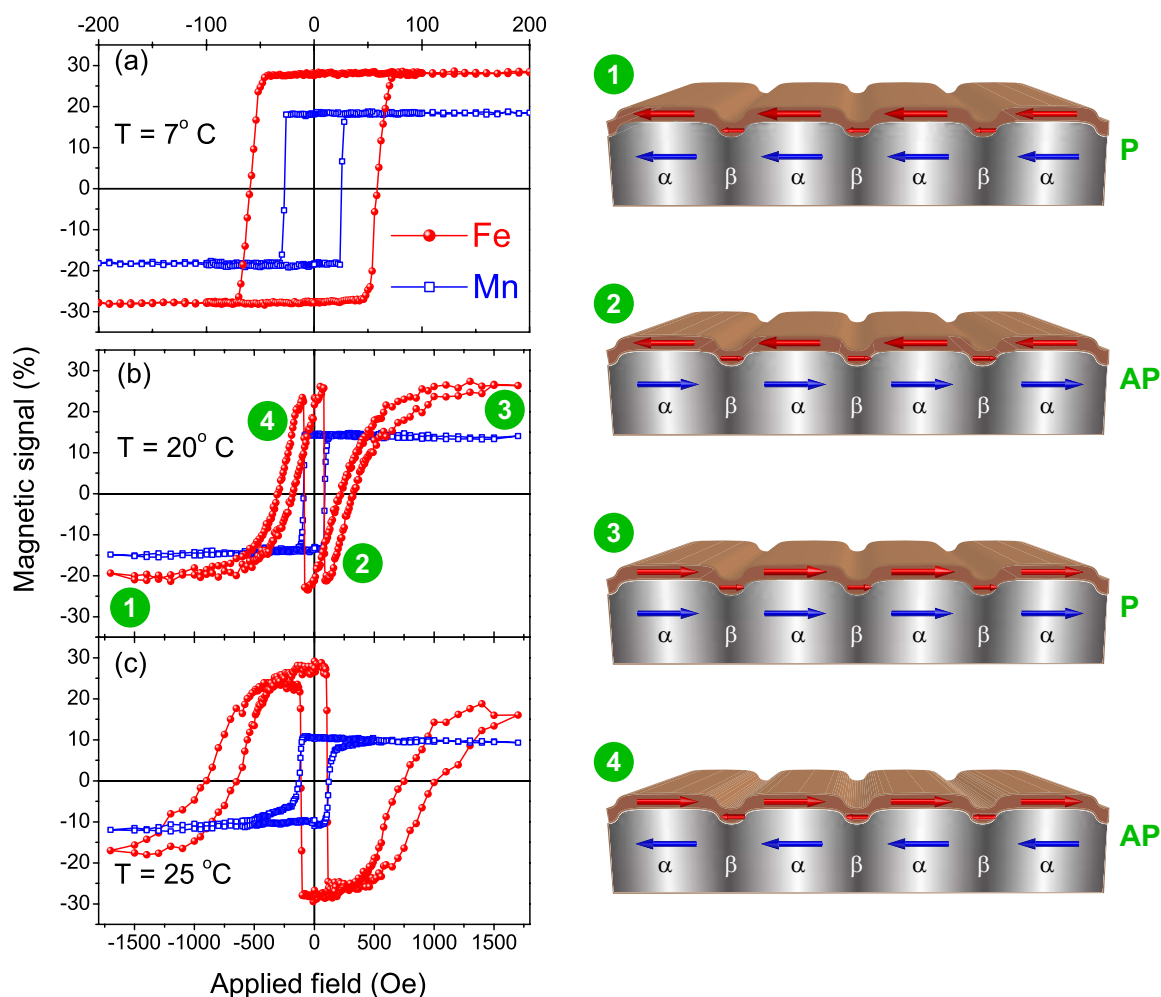


Figure 1 | Element selective hysteresis loops in Fe_{3nm}/MnAs_{200nm}/GaAs(001). Specular reflectivity is recorded at 7°C (a), 20°C (b) and 25°C (c), using circularly polarized x-rays whose energy is tuned either to the Mn (□) or to the Fe (●) 2p resonance. The magnetic signal is expressed as a percentage variation with respect to the average value over a cycle. Note the different field scales for (a) and (b), (c). The Fe and MnAs magnetic configurations corresponding to four field values in panel (b) are depicted on the right.



magnetizations. The coercive fields for Fe and Mn are very different (58 and 27 Oe, respectively), indicating that there is a weak interface coupling, if any at all^{32,34}. Figs. 1b ($T = 20^\circ\text{C}$) and 1c ($T = 25^\circ\text{C}$) show that, when α/β stripes form, the shape of the Fe hysteresis loop is strongly modified: much higher fields are required to reach saturation and the remanent magnetization is now antiparallel (AP) with respect to MnAs.

A schematic interpretation of these element selective hysteresis curves is sketched in Fig. 2. Over the phase-coexistence temperature range, finite-size ferromagnetic α -MnAs stripes form with their easy magnetization direction along the short side of the stripe^{11,19,20,32}. The effective magnetic field H_{eff} felt by Fe on top of α -MnAs stripes is the sum of the bias external field H_{ext} and of a dipolar term H_{D} (proportional to the MnAs magnetization) generated by the underlying ferromagnetic stripe. Analytical estimates of H_{D} (Fig. 2a) yield values that largely exceed the coercive field of Fe. The change in the Mn magnetization sign at the coercive field of MnAs inverts the sign of the H_{D} contribution to H_{eff} ; as a result, the Fe magnetization dependence on H_{ext} (Fig. 2b) shows two displaced loops, the side displacement providing a rough estimate of H_{D} . According to Fig. 1b, c, H_{D} values are ~ 300 and ~ 800 Oe at 20 and 25°C , respectively. This compares well with previous experiments^{32,34}.

Surface dipolar fields as sketched in Fig. 2 can be tuned by acting on the MnAs α/β micromagnetic structure via temperature control. Fig. 3 shows the result of a 0 – 18°C thermal cycle performed in zero field, following a bias pulse ($H_{\text{ext}} = +300$ Oe) that sets the initial P alignment of the Fe and MnAs magnetizations. The Mn signal is barely affected during the thermal cycle, with only a slight decrease at high temperature due both to α -MnAs magnetization reduction and to the formation of paramagnetic β -MnAs, and it regains its initial value at the end of the cycle. The Fe magnetization, on the contrary, varies rapidly above 12°C , inverts its sign at $\sim 15^\circ\text{C}$, and then keeps it until the end of the cycle. The remanent AP alignment observed in the phase coexistence region (Figs. 1b, c) persists upon cooling, showing that, at low-temperature, the system is bi-stable with two (P or AP) possible magnetic configurations¹¹. The mechanism driving the Fe magnetization reversal is the same as depicted in Fig. 2. Below $\sim 12^\circ\text{C}$, Fe rests on a flat and homogeneously α -phase MnAs template, keeping the remanent P configuration imposed by the H_{ext} pulse. As the temperature increases, the dipolar field H_{D}

generated by the finite size α -stripes exceeds the Fe coercive field, switching its magnetization direction. Due to the weak coupling between Fe and MnAs (see Fig. 1a), the two layers maintain the AP configuration when the system is cooled down again.

Magnetic configuration vs. T_{max} . Having confirmed that TIMS occurs in our Fe/MnAs/GaAs(001) samples, with the Fe magnetization changing sign in a ($T_{\text{min}}-T_{\text{max}}$) thermal cycle, we move now to the central topic of this investigation, i.e. the analysis of the role played by T_{max} on the final magnetic configuration. Fig. 4 compares, for sample B, the evolution of the Fe magnetic signal in thermal cycles with different T_{max} between 11.8°C (just below the onset of the $\alpha \rightarrow \beta$ transition) and 64.8°C (well above the complete transition to the β -phase). The lowest T_{max} of 11.8°C (Fig. 4a) does not promote any phase transformation, therefore it leaves the Fe signal unaffected and both the Fe and the MnAs recover their initial P magnetic state at the end of the cycle. A slight increase of T_{max} up to 16.8°C (Fig. 4b) produces already a complete reversal at the end of the cycle, analogous to that reported in Fig. 3 for sample A. The dashed vertical line in Fig. 4 illustrates the existence of a threshold temperature value for TIMS in Fe, corresponding to the onset of the α/β phase coexistence. The thermal cycles in Fig. 4c–e show that a complete reversal of the Fe magnetization with final AP alignment is obtained for T_{max} values up to approximately 28°C , i.e. well into the temperature range of the $\alpha \rightarrow \beta$ transformation. The process seems to work efficiently as long as α -MnAs retains the magnetization alignment imposed by the initial bias field pulse, prior to thermal cycling. It is known, however, that when the α -MnAs stripes shrink as the temperature increases, their internal magnetic structure is dominated by complex domain patterns, including out-of-plane components^{31,39–42}. In Fig. 4, the dotted line at 29°C identifies the temperature value that corresponds to equal width α and β stripes, as determined by x-ray diffraction: one remarks that above this value the overall Fe reversal efficiency decreases rapidly (Fig. 4e, f).

Once T_{max} exceeds 40°C (Fig. 4g), complete transformation to the paramagnetic β -phase has taken place. As the phase-coexistence temperature range is crossed during the cool-down branch of the cycle, magnetization alignment in the α -MnAs stripes is no longer homogeneous and breaks up into domains with opposite orienta-

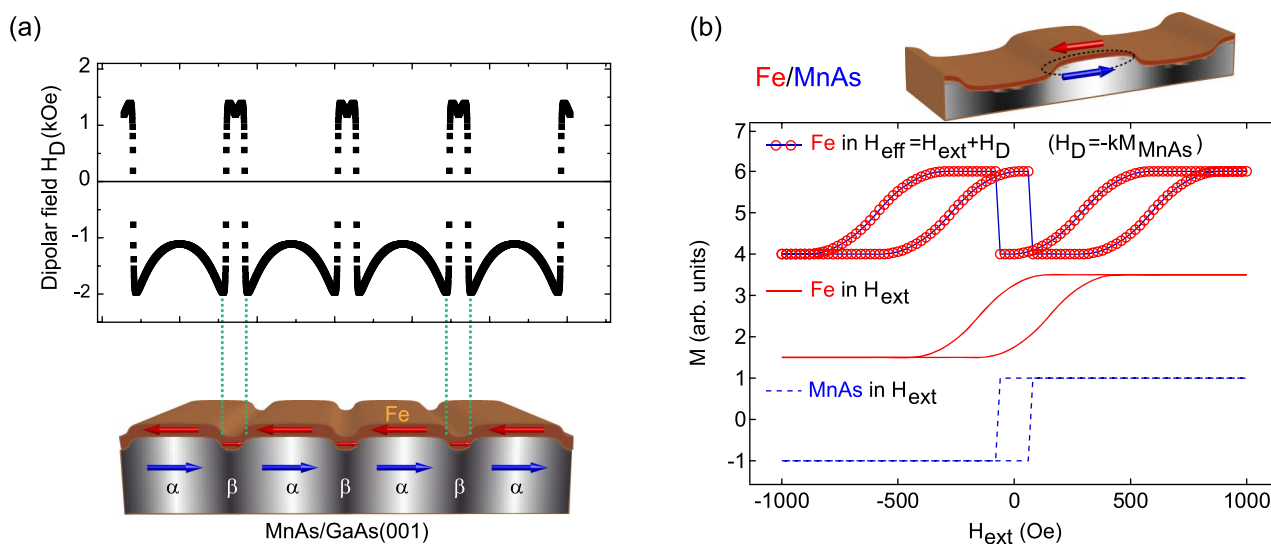


Figure 2 | Schematic description of the Fe hysteresis loop in presence of α/β MnAs stripes. (a): finite size α -stripes magnetized along their short side generate a surface dipolar field H_{D} , proportional to the MnAs magnetization, that we estimate analytically. (b): H_{D} adds to the external bias field H_{ext} to determine the effective field H_{eff} acting on the Fe overlayer. The hysteresis loop that Fe would display in absence of dipolar fields (—) shifts according to the value of H_{D} (○), whose sign changes with the MnAs magnetization (---), i.e., at the MnAs coercive field. Notice that the Fe and MnAs hysteresis loops in (b) are for an illustrative purpose only and their shapes do not compare to any experimental condition specifically.

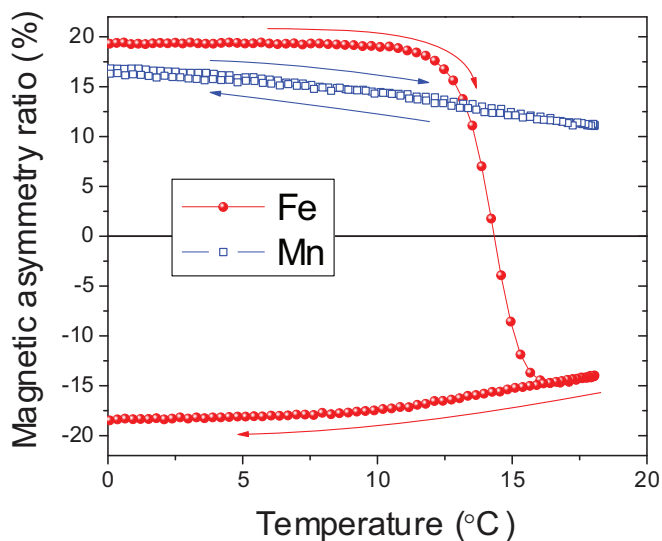


Figure 3 | Thermally induced magnetisation switching in $\text{Fe}_{3\text{nm}}/\text{MnAs}_{200\text{nm}}/\text{GaAs}(001)$. Specular x-ray reflectivity at the Fe-2p (●) and Mn-2p (□) resonances, measured in a thermal cycle with $T_{\text{max}} = 18^\circ\text{C}$. The magnetic signal is defined as the difference between two measurements performed for opposite x-ray helicities, divided by their sum.

tions. Across the phase-coexistence temperature region, surface dipolar fields still drive the Fe magnetization to align AP to the underlying α -MnAs locally, but the disordered distribution of the α -MnAs domains leads, at the end of the cycle, to a much reduced net Fe magnetization, whose exact value is difficult to predict.

Thermal cycles with a bias field. The strong dependence of the final magnetic configuration on T_{max} represents a major drawback for the Fe/MnAs/GaAs(001) system as far as TIMS applications are concerned. This is particularly true if the goal is to induce fast and local switching by using short and focused laser pulses. They induce large, spatially inhomogeneous and time-dependent temperature variations^{36,37}, making it very difficult to predict T_{max} . In the following, we deal with the effect that an external bias field H_{ext} has on attaining predictable and well-ordered magnetization states at the end of a high-temperature cycle.

Fig. 5 shows that thermal cycles with $T_{\text{max}} 60^\circ\text{C}$ stabilize sample B in various low temperature magnetic configurations, as a function of the bias field. At $H_{\text{ext}} = 0$ (Fig. 5a), the result is similar to that reported for sample A in Fig. 4g, i.e. a final state with AP coupling but strongly reduced Fe and MnAs net magnetizations.

Applying $H_{\text{ext}} = +45$ Oe, i.e. a bias field larger than the α -MnAs coercive field but smaller than that of Fe, the MnAs magnetization is fully recovered at the end of the cycle, while the Fe magnetization has changed sign (Fig. 5b). The role of this weak bias field is particularly significant during the cooling branch of the cycle, when, going below 40°C , it orders the magnetization of the emerging α -MnAs phase. Then the surface dipolar field generated by the α -MnAs stripes (Fig. 2) orient the magnetization of the Fe overlayer AP. Since the bias field is lower than the Fe coercive field, the AP alignment is kept also at low temperature, until the end of the cycle. For bias field values between 40 and 50 Oe, we obtain systematically the Fe magnetization switching.

When H_{ext} is larger than the ~ 75 Oe Fe saturation field (see Fig. 1a), the Fe magnetization undergoes two sign changes during the cooling branch of the thermal cycle (Fig. 5c). Above 40°C , Fe sits on a homogeneous β -phase template and the bias field is large enough to saturate its magnetization. In the phase coexistence region, between 40°C and $\sim 15^\circ\text{C}$, the surface dipolar fields generated by the α -MnAs stripes largely overcome the bias field and impose an Fe/

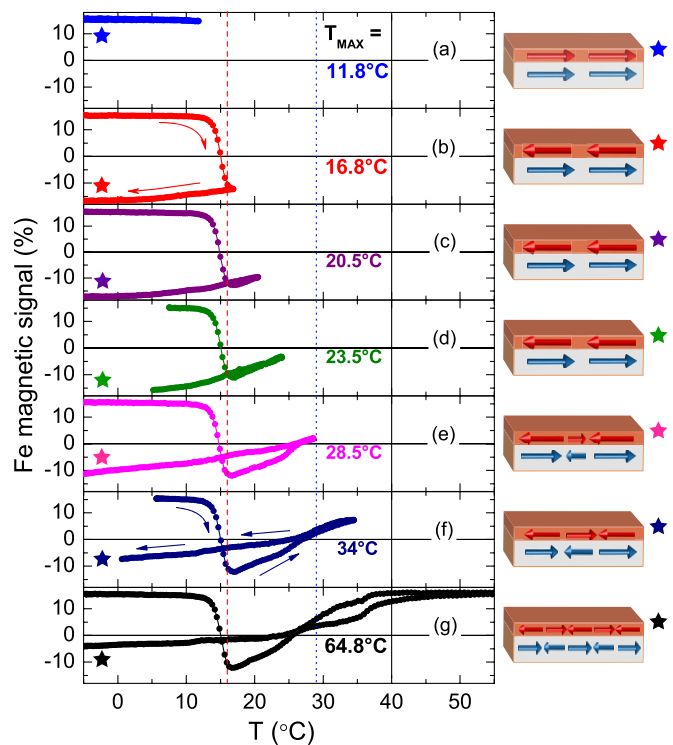


Figure 4 | Magnetic configuration vs. T_{max} . Temperature dependent Fe magnetic signal in $\text{Fe}_{5\text{nm}}/\text{MnAs}_{140\text{nm}}/\text{GaAs}(001)$, recorded during thermal cycles with T_{max} ranging from 11.8°C (a) to 64.8°C (g). Vertical lines locate the threshold temperature for Fe TIMS ($\sim 15^\circ\text{C}$, - - -), the temperature corresponding to α and β stripes of equal width ($\sim 29^\circ\text{C}$,), and the temperature for completing the transition to the β -MnAs phase (40°C , —). A sketch of the final Fe and MnAs magnetic configurations is shown for each cycle.

MnAs AP alignment, as discussed above. When the temperature is lowered further, the template turns into a homogeneous α -phase and the dipolar fields vanish, allowing the bias field to orient the Fe magnetization along its original direction, parallel to that of MnAs.

Discussion

Let us first place our results in the context of the on-going research in this field. TIMS at ambient temperatures was reported recently in the case of SmFeO_3 single crystals³, a compound that shows a canted antiferromagnetic ordering with associated weak values of the magnetization. Switching was accomplished by exploiting the temperature and field dependence of a spin reorientation transition of the Fe sublattice. In the present work, we make use of a composite structure to control magnetization switching in a metallic Fe thin film, a material with a larger magnetization. Moreover, as shown in Fig. 5, the magnetic configuration of the system can be selected by adjusting the applied field over a range of moderate values, smaller than 100 Oe. Turning to thermally assisted magnetic recording, the main idea is that the coercive field can be lowered below a critical value (the external field) by increasing the temperature. Our approach is different, in the sense that we use temperature to control the effective field acting on the overlayer. Finally, it should be pointed out that a major asset of the Fe/MnAs epitaxial system is that it can easily be integrated into GaAs-based technology.

Our element selective magnetization measurements provide information on TIMS in Fe/MnAs/GaAs(001) on three different levels. First, they confirm that we have at our disposal a thin film epitaxial system featuring two local stable magnetic configurations (P and AP) and that we can switch from one to the other by a thermal cycle of a few degrees close to ambient temperature (Fig. 3). Second,

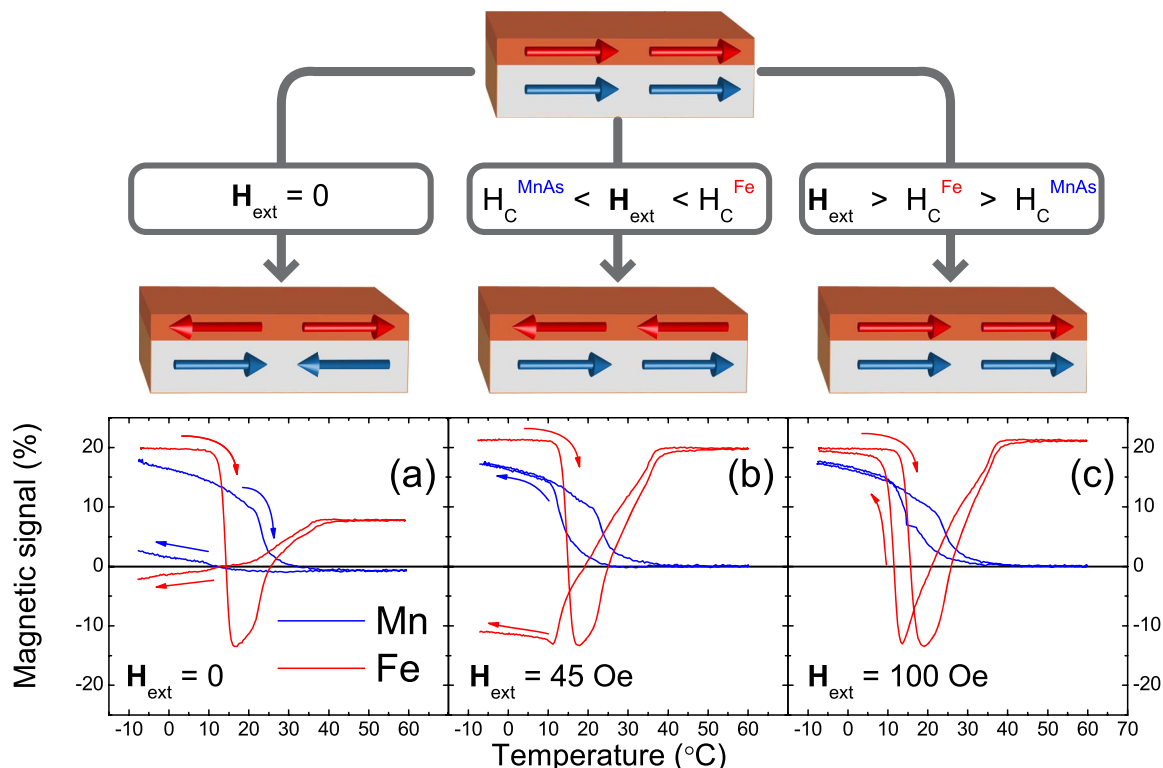


Figure 5 | Thermal cycles with a bias field. Fe (—) and Mn (—) magnetic signals in thermal cycles with bias field: (a) $H_{\text{ext}} = 0$, (b) $H_{\text{ext}} = +45$ Oe, (c) $H_{\text{ext}} = +100$ Oe. For all cycles, a +300 Oe pulse set the parallel initial state between Fe and MnAs magnetizations and T_{max} is 60°C. The sample structure is $\text{Fe}_{3\text{nm}}/\text{MnAs}_{200\text{nm}}/\text{GaAs}(001)$. The final magnetic configuration after the thermal cycle is indicated above each figure: a disordered state with local antiparallel alignment is obtained at remanence (a), while a bias field value in between the coercive fields of Fe and MnAs (b) or larger than both (c) produces a final state with antiparallel or parallel alignment between the Fe and MnAs magnetizations, respectively.

they show that the maximum temperature T_{max} reached during the cycle strongly affects the final magnetic configuration (Fig. 4); this T_{max} dependence is a potential inconvenience that can hamper the achievement of reproducible results by TIMS. Finally, we demonstrate that it is possible to bypass these difficulties relating to T_{max} by applying a bias field during the thermal cycle; the choice of the bias field value determines the final Fe/MnAs configuration: ordered P (Fig. 5c), ordered AP (Fig. 5b) or disordered with local AP coupling (Fig. 5a).

The use of an element-selective magnetization probe such as resonant x-ray scattering plays an important part in this investigation, since it allows us to disentangle Fe and MnAs contributions to the complex magnetic behaviour of the Fe/MnAs system, as a function of temperature and field. Once the mechanisms underlying the magnetic response are understood, the more conventional magnetometry techniques can be applied with greater confidence. Low temperature (α -MnAs phase) and high temperature (β -MnAs phase) hysteresis loops will probe respectively the magnetization of both Fe and MnAs layers together or of Fe separately, while at intermediate temperatures data must be interpreted according to the scheme depicted in Fig. 2.

Our work confirms that the control of the template surface dipolar fields is an interesting way of acting on the overlayer magnetization, with a potential for temperature-driven magnetization switching without applying external fields. Our results on the Fe/MnAs/GaAs(001) epitaxial system, also show, however, that the maximum temperature reached in the thermal cycle affects the final magnetic configuration, thus hindering possible applications, in particular those based on the use of a laser pulse for controlling the temperature^{35–37}. This calls for two comments.

A general comment first is that this approach towards TIMS is not limited to the specific material illustrated here, as the basic idea is that

it is possible to modulate a substrate-generated dipolar field by controlling the temperature¹⁰. An alternative to the self-organisation of ferromagnetic and paramagnetic stripes in MnAs/GaAs(001) would be to create a well-defined spatial modulation of T_{C} in a ferromagnetic substrate, either by ion implantation or by chemical doping. These systems can be designed so that they do not suffer from the T_{max} dependence of TIMS encountered in MnAs.

The second comment, more specific to the Fe/MnAs system, is that coupling thermal cycles to the presence of a weak bias field stabilizes selected magnetic configurations in a predictable way, at a given temperature, regardless of T_{max} . In this case, we no longer achieve magnetization control by acting on the temperature only, since an external field is required. The process, though, retains potential for applications, especially in view of using laser pulses for achieving temperature control. Magnetization switching can be triggered by a short (~ 100 fs) laser pulse even though the temperature driven process is likely to take place over a timescale of several ns. In the case of a sample immersed in a weak homogeneous non-local bias field, the laser pulse will bring the temperature well above the phase transition in MnAs, modifying the surface dipolar field and altering the Fe magnetization only locally over the irradiated area. The final magnetic configuration will depend on the bias field strength and orientation, in a process similar to thermally assisted magnetization reversal⁴⁵, yet with the dipolar field generated by the substrate enhancing the effective magnetic field acting on the overlayer.

Methods

The samples were prepared at the Institut des NanoSciences de Paris, following the same molecular beam epitaxy procedure detailed before³². The GaAs(001) epi-ready wafer was first annealed at about 600°C in an As flux to remove oxides, and a GaAs buffer layer was grown to obtain an atomically flat surface. Then the wafer was cooled to 450°C under As flux in order to form an As-terminated $c(4 \times 4)$ surface. After reducing the sample temperature to 230°C, the MnAs layer was grown according to



the procedure described by Tanaka *et al.*¹⁹ to obtain films with A-type orientation, as confirmed *in situ* by electron diffraction and *ex situ* by x-ray diffraction analysis. The sample was then transferred under ultrahigh vacuum to a separate chamber where the Fe layer was deposited using a Knudsen cell, with the MnAs template at 160°C. *In situ* electron diffraction and *ex situ* transmission electron microscopy show that Fe grows epitaxially on MnAs³². Finally, a capping layer (either ZnSe or Au) was deposited for protection against contamination.

The results reported here refer to two samples with the structure ZnSe_{5nm}/Fe_{3nm}/MnAs_{200nm}/GaAs(001) (sample A) and Au_{5nm}/Fe_{5nm}/MnAs_{140nm}/GaAs(001) (sample B). In spite of the different thicknesses and capping layers, both display the same behavior as far as our investigation is concerned. At room temperature, they feature well-ordered α/β stripes with periods of ~ 1340 (A) and ~ 1030 nm (B), which match well the expected values²².

Synchrotron-based x-ray resonant scattering measurements took place at the Circular Polarization beamline of the ELETTRA storage ring (Trieste, Italy), using the vertical-scattering-plane IRMA reflectometer⁴⁴. Over the 630–730 eV photon energy range used in our experiment, the beamline provides a circular polarization rate of $\sim 70\%$ for both helicities (electromagnetic undulator source) and an energy resolving power of ~ 2500 . The sample temperature, read by a thermo-resistance, was set over the 0°C–80°C range using a Peltier thermoelectric device driven by a temperature controller. An electromagnet could apply static fields up to 500 Oe (1.7 kOe pulsed) along the easy magnetization direction of α -MnAs, that was aligned parallel to the intersection between the sample surface and the scattering plane. The scattered intensity was measured using a slitted photodiode (0.08° acceptance within the scattering plane). Rocking scans were collected for assessing the stripe period and the temperature dependent α/β ratio²⁴. All x-ray specular reflectivity data reported in this work were collected at a scattering angle of 16°. This provided a convenient compromise between high reflectivity and large magnetic signals. External field dependent magnetic signals (hysteresis loops of Fig. 1) were collected using a single photon helicity; the magnetic signal is defined as the difference between the reflectivity at each point and the average over a complete loop, divided by the average. Temperature dependent magnetic signals (Figs. 3, 4 and 5) correspond to the difference between two measurements performed for opposite photon helicities, divided by their sum.

- Lahtinen, T. H. E., Franke, K. J. A. & van Dijken, S. Electric-field control of magnetic domain wall motion and local magnetization reversal. *Sci. Rep.* **2**, 258 (2012).
- Wang, L. *et al.* Electric control of magnetism at room temperature. *Sci. Rep.* **2**, 223 (2012).
- Slonczewski, J. C. Current-driven excitation of magnetic multilayers. *J. Magn. Magn. Mater.* **159**, L1 (1996).
- Yang, T., Kimura, T. & Otani, Y. Giant spin-accumulation signal and pure spin-current-induced reversible magnetization switching. *Nature Phys.* **4**, 851 (2008).
- Yuan, S. J. *et al.* Spin switching and magnetization reversal in single-crystal NdFeO₃. *Phys. Rev. B* **87**, 184405 (2013).
- Cao, S., Zhao, H., Kang, B., Zhang, J. & Ren, W. Temperature induced spin switching in SmFeO₃ single crystal. *Sci. Rep.* **4**, 5960 (2014).
- Kimel, A. V., Kirilyuk, A., Tsvetkov, A., Pisarev, R. V. & Rasing, T. Laser-induced ultrafast spin reorientation in the antiferromagnet TmFeO₃. *Nature* **429**, 850 (2004).
- Stanciu, C. D. *et al.* Subpicosecond magnetization reversal across ferrimagnetic compensation points. *Phys. Rev. Lett.* **99**, 217204 (2007).
- Hassdenteufel, A. *et al.* Thermally assisted all-optical helicity dependent magnetic switching in amorphous Fe_{1-x}Tb_x alloy films. *Adv. Mater.* **25**, 3122 (2013).
- Marangolo, M. & Sacchi, M. Method for changing the direction of magnetization in a ferromagnetic layer. *French patent n. 2947375, U.S. patent pending.*
- Sacchi, M. *et al.* Thermal switching of the magnetization in an iron film on a magnetically active template MnAs/GaAs(001). *Phys. Rev. B* **81**, 240801 (2010).
- Bean, C. P. & Rodbell, D. S. Magnetic Disorder as a First-Order Phase Transformation. *Phys. Rev.* **126**, 104 (1962).
- Menyuk, N., Kafalas, J. A., Dwight, K. & Goodenough, J. B. *Phys. Rev.* **177**, 942 (1969).
- Pytlík, L. & Zieba, A. Magnetic phase diagram of MnAs. *J. Magn. Magn. Mater.* **51**, 199 (1985).
- Wada, H. & Tanabe, Y. Giant magnetocaloric effect of MnAs_{1-x}Sb_x. *Appl. Phys. Lett.* **79**, 3302 (2001).
- Tegus, O., Brück, E., Buschow, K. H. J. & de Boer, F. R. Transition-metal-based magnetic refrigerants for room-temperature applications. *Nature* **415**, 150 (2002).
- Mosca, D. H., Vidal, F. & Etgens, V. H. Strain engineering of the magnetocaloric effect in MnAs epilayers. *Phys. Rev. Lett.* **101**, 125503 (2008).
- Duquesne, J.-Y. *et al.* Ultrasonic triggering of giant magnetocaloric effect in MnAs thin films. *Phys. Rev. B* **86**, 035207 (2012).
- Tanaka, M. *et al.* Epitaxial orientation and magnetic properties of MnAs thin films grown on (001) GaAs: Template effects. *Appl. Phys. Lett.* **65**, 1964 (1994).
- Däweritz, L. Interplay of stress and magnetic properties in epitaxial MnAs films. *Rep. Prog. Phys.* **69**, 2581 (2006).
- Kaganer, V. M. *et al.* Strain-mediated phase coexistence in MnAs heteroepitaxial films on GaAs: An x-ray diffraction study. *Phys. Rev. B* **66**, 045305 (2002).
- Vidal, F. *et al.* Tuning the period of elastic MnAs/GaAs(001) α - β pattern by Fe deposition. *Appl. Phys. Lett.* **97**, 251914 (2010).
- Breitwieser, R. *et al.* Phase transition and surface morphology of MnAs/GaAs(001) studied with in situ variable-temperature scanning tunneling microscopy. *Phys. Rev. B* **80**, 045403 (2009).
- Magalhães-Paniago, R. *et al.* X-ray method to study temperature-dependent stripe domains in MnAs/GaAs(001). *Appl. Phys. Lett.* **86**, 053112 (2005).
- Wellmann, P. J., Garcia, J. M., Feng, J.-L. & Petroff, P. M. Giant magnetoresistance in a low-temperature GaAs/MnAs nanoscale ferromagnet hybrid structure. *Appl. Phys. Lett.* **73**, 3291 (1998).
- Tanaka, M., Saito, K. & Nishinaga, T. Epitaxial MnAs/GaAs/MnAs trilayer magnetic heterostructures. *Appl. Phys. Lett.* **74**, 64 (1999).
- Stephens, J. *et al.* Spin accumulation in forward-biased MnAs/GaAs Schottky diodes. *Phys. Rev. Lett.* **93**, 097602 (2004).
- García, V. *et al.* Spectroscopic measurement of spin-dependent resonant tunneling through a 3D disorder: the case of MnAs/GaAs/MnAs junctions. *Phys. Rev. Lett.* **97**, 246802 (2006).
- Nowakowski, M. E., Fuchs, G. D., Mack, S., Samarth, N. & Awschalom, D. D. Spin control of drifting electrons using local nuclear polarization in ferromagnet-semiconductor heterostructures. *Phys. Rev. Lett.* **105**, 137206 (2010).
- Jahangir, S., Doğan, F., Kum, H., Manchon, A. & Bhattacharya, P. Spin diffusion in bulk GaN measured with MnAs spin injector. *Phys. Rev. B* **86**, 035315 (2012).
- Coelho, L. N. *et al.* Magnetic reconfiguration of MnAs/GaAs(001) observed by magnetic force microscopy and resonant soft x-ray scattering. *J. Appl. Phys.* **100**, 083906 (2006).
- Sacchi, M. *et al.* Uniaxial anisotropy and temperature driven magnetization reversal of Fe deposited on a MnAs/GaAs(001) magnetic template. *Phys. Rev. B* **77**, 165317 (2008).
- Spezzani, C. *et al.* Soft x-ray magneto-optics: probing magnetism by resonant scattering experiments. *IEEE Trans. Mag.* **49**, 4711 (2013).
- Breitwieser, R. *et al.* Imaging the antiparallel magnetic alignment of adjacent Fe and MnAs thin films. *Appl. Phys. Lett.* **93**, 122508 (2008).
- Sacchi, M. *et al.* Time resolved pump-probe scattering in MnAs/GaAs(001): a first look into the dynamics of α - β stripe domains. *Appl. Phys. Lett.* **100**, 211905 (2012).
- Dean, J. J., Rench, D. W., Samarth, N. & van Driel, H. M. Domain dynamics in thin solid films following ultrashort pulse excitation. *Phys. Rev. Lett.* **111**, 035701 (2013).
- Dean, J. J., Lange, C. & van Driel, H. M. Ultrafast surface strain dynamics in MnAs thin films observed with second harmonic generation. *Phys. Rev. B* **89**, 024102 (2014).
- Sacchi, M. *et al.* Soft-x-ray resonant scattering from V/Fe (001) magnetic superlattices. *Phys. Rev. B* **60**, 12569(R) (1999).
- Plake, T. *et al.* Temperature-dependent magnetic force microscopy investigation of epitaxial MnAs films on GaAs(001). *Appl. Phys. Lett.* **82**, 2308 (2003).
- Ney, A. *et al.* Magnetic out-of-plane component in MnAs/GaAs(001). *Appl. Phys. Lett.* **83**, 2850 (2003).
- Engel-Herbert, R. *et al.* Understanding the submicron domain structure of MnAs thin films on GaAs(001): Magnetic force microscopy measurements and simulations. *Appl. Phys. Lett.* **84**, 1132 (2004).
- Engel-Herbert, R., Hesjedal, T. & Schaadt, D. M. Three-dimensional micromagnetic domain structure of MnAs films on GaAs(001): experimental imaging and simulations. *Phys. Rev. B* **75**, 094430 (2007).
- Thiele, J.-U., Maat, S. & Fullerton, E. E. FeRh/FePt exchange spring films for thermally assisted magnetic recording media. *Appl. Phys. Lett.* **82**, 2859 (2003).
- Sacchi, M. *et al.* Ultra-high vacuum soft X-ray reflectometer. *Rev. Sci. Instrum.* **74**, 2791 (2003).

Acknowledgments

We thank ELETTRA Sincrotrone Trieste for granting beamtime to our project and the Circular Polarization beamline staff for providing technical assistance during the experiment. We are grateful to Coryn F. Hague (LCPMR, Paris) for his comments and suggestions.

Author contributions

C.S., M.M. and M.S. conceived the experiment. M.E. and V.H.E. prepared and characterized the samples. C.S., R.D., H.P. and M.S. performed the measurements. F.V., M.M. and M.S. analyzed the data and wrote the manuscript. All authors contributed to the manuscript and to the interpretation of the data.

Additional information

Competing financial interests: The authors declare no competing financial interests.

How to cite this article: Spezzani, C. *et al.* Thermally induced magnetization switching in Fe/MnAs/GaAs(001): selectable magnetic configurations by temperature and field control. *Sci. Rep.* **5**, 8120; DOI: 10.1038/srep08120 (2015).



This work is licensed under a Creative Commons Attribution-NonCommercial-ShareAlike 4.0 International License. The images or other third party material in this article are included in the article's Creative Commons license, unless indicated otherwise in the credit line; if the material is not included under the Creative

Commons license, users will need to obtain permission from the license holder in order to reproduce the material. To view a copy of this license, visit <http://creativecommons.org/licenses/by-nc-sa/4.0/>